Received: 22 March 2017 | Revised: 9 May 2017 | Accepted: 8 June 2017

DOI: 10.1002/cne.24267

RESEARCH ARTICLE

WILEY The Journal of Comparative Neurology

Congenital deafness affects deep layers in primary and secondary auditory cortex

Christoph Berger[1] | Daniela Kühne[1] | Verena Scheper[1] | Andrej Kral[1,2]

[1]Institute of AudioNeuroTechnology & Department of Experimental Otology, ENT Clinics, School of Medicine, Hannover Medical University, Hannover, Germany

[2]School of Behavioral and Brain Sciences, The University of Texas, Dallas, USA

Correspondence
A. Kral, Department of Experimental Otology, Stadtfelddamm 34, 30625 Hannover, Germany.
Email: kral.andrej@mh-hannover.de

Abstract

Congenital deafness leads to functional deficits in the auditory cortex for which early cochlear implantation can effectively compensate. Most of these deficits have been demonstrated functionally. Furthermore, the majority of previous studies on deafness have involved the primary auditory cortex; knowledge of higher-order areas is limited to effects of cross-modal reorganization. In this study, we compared the cortical cytoarchitecture of four cortical areas in adult hearing and congenitally deaf cats (CDCs): the primary auditory field A1, two secondary auditory fields, namely the dorsal zone and second auditory field (A2); and a reference visual association field (area 7) in the same section stained either using Nissl or SMI-32 antibodies. The general cytoarchitectonic pattern and the area-specific characteristics in the auditory cortex remained unchanged in animals with congenital deafness. Whereas area 7 did not differ between the groups investigated, all auditory fields were slightly thinner in CDCs, this being caused by reduced thickness of layers IV–VI. The study documents that, while the cytoarchitectonic patterns are in general independent of sensory experience, reduced layer thickness is observed in both primary and higher-order auditory fields in layer IV and infragranular layers. The study demonstrates differences in effects of congenital deafness between supragranular and other cortical layers, but similar dystrophic effects in all investigated auditory fields.

KEYWORDS

cortical column, cochlear implant, development, hearing loss, higher-order areas, infragranular layers, RRID: AB_509997

1 | INTRODUCTION

Congenital deafness affects the development of the auditory cortex and leads to many functional deficits that can be compensated for by neurosensory restoration using cochlear implants within an early critical period (Kral & Sharma, 2012). While developmental critical periods have been described both in humans and in animal models, the reasons for closure of sensitive periods are multifactorial (Kral, 2013). Despite abundant data on the effects of congenital deafness on the primary auditory cortex, little information has been obtained about auditory fields beyond the primary processing level (secondary and tertiary, here referred to as 'higher-order'; Figure 1; see Lee & Winer, 2011). Since higher-order fields are crucial for perception (Rubin, Ulanovsky, Nelken, & Tishby, 2016; Griffiths & Warren, 2004), it is of essential importance to understand their fate in congenital deafness.

Dystrophic changes affecting cells and synapses in the 'deaf' auditory pathway, including smaller soma size and restructured synaptic morphology, have been reported in many studies involving different species, including congenitally deaf cats (CDCs) (O'Neil, Limb, Baker, & Ryugo, 2010; Redd, Cahill, Pongstaporn, & Ryugo, 2002; Ryugo, Rosenbaum, Kim, Niparko, & Saada, 1998; Saada, Niparko, & Ryugo, 1996; Sento & Ryugo, 1989) and pharmacologically neonatally deafened cats (Hultcrantz, Snyder, Rebscher, & Leake, 1991; Leake, Snyder, Hradek, & Rebscher, 1995; Lustig, Leake, Snyder, & Rebscher, 1994; Hardie, Martsi-McClintock, Aitkin, & Shepherd, 1998; Hardie & Shepherd, 1999; Fallon, Irvine, & Shepherd, 2008). Using retrograde tracers, the

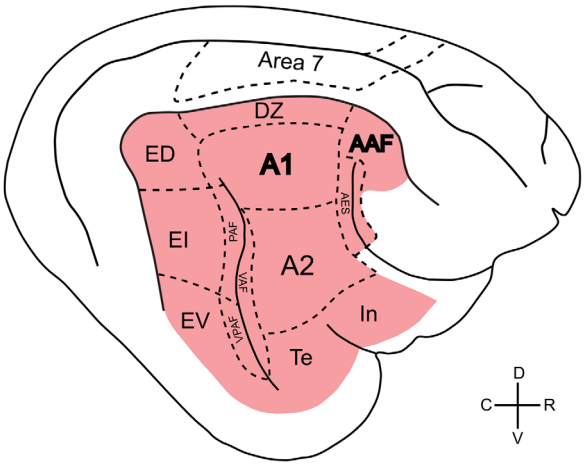

FIGURE 1 Schematic illustration of the cortical auditory fields in the feline brain, shown in red. The visual area 7, used as a control for the present experiments, is additionally shown. Dashed lines indicate the approximate average position of the field borders. Primary auditory fields are A1 and AAF (label bold), the remaining areas are higher-order secondary or tertiary fields. A1: primary auditory field; AAF: anterior auditory field; AES: field of the anterior ectosylvian sulcus; A2: secondary auditory field; DZ: dorsal zone; ED: dorsal division of the posterior ectosylvian field; EI: intermediate division of the posterior ectosylvian field; EV: ventral division of the posterior ectosylvian field; PAF: posterior auditory field; Te: temporal auditory field; In: insular auditory field; VAF: ventral auditory field; VPAF: ventroposterior auditory field

patterns of cortical inputs have been examined in hearing and CDCs (Barone, Lacassagne, & Kral, 2013; Butler et al., 2017). In CDCs the predominant anatomical inputs remained auditory in both the primary auditory cortex (field A1) and the secondary field (dorsal zone, DZ; Barone et al., 2013). However, a moderate number of new ectopic projections have been observed from visual, somatosensory, and multimodal brain regions to field DZ (Barone et al., 2013). Retrograde tracers placed in another secondary field—the posterior auditory field (PAF) of CDCs (Butler, Chabot, Kral, & Lomber, 2017)—revealed similar moderate changes that closely matched the observations in DZ. This has been further supported by studies on early deafened cats (e.g., Butler, Chabot, & Lomber, 2016; Kok, Chabot, & Lomber, 2014; Meredith, Clemo, Corley, Chabot, & Lomber, 2015). Taken together, anatomical cortical reorganization in deaf animals is moderate and both the corticocortical and thalamocortical projections are largely conserved.

On the other hand, extensive functional deficits in primary cortical field A1 of deaf animals (Hartmann, Shepherd, Heid, & Klinke, 1997; Raggio & Schreiner, 1999; Fallon et al., 2014; Fallon, Irvine, & Shepherd, 2009; Tillein et al., 2010, 2016; Beitel, Vollmer, Raggio, & Schreiner, 2011; review in Kral & Sharma, 2012) indicate a dichotomy between deficient neuronal function and preserved fiber tracts to A1, and point to a synaptic or cellular origin of the functional deficits (Kral et al., 2017). A similar dichotomy between generally preserved anatomical fiber tracts and extensive functional deficits following sensory deprivation has been noted previously in the visual system (Mower, Caplan, Christen, & Duffy, 1985).

It remains unclear whether deficits as described in field A1 also involve higher-order fields. While it has been shown that auditory responsiveness is preserved in field DZ of CDCs along with increased visual responsiveness (Land et al., 2016), the only previous direct comparison between two cortical hierarchical levels (primary vs. secondary) relates to connection patterns (Barone et al., 2013). Furthermore, cortical minicolumns, the smallest functional unit in the cerebral cortex (Mountcastle, 1997), have been investigated functionally and deficits in columnar activation patterns were described in field A1 of CDCs (Kral, Hartmann, Tillein, Heid, & Klinke, 2000; Kral, Tillein, Heid, Hartmann, & Klinke, 2005). The consequences of these deficits for the anatomy of the cortical columns remain unclear.

Finally, in previous studies, field specificity in the capacity for cross-modal takeover following congenital deafness has been documented: visual cross-modal function was demonstrated in secondary fields DZ and PAF in CDCs (Lomber, Meredith, & Kral, 2010; Land et al., 2016), but not in primary fields A1 and anterior auditory field (AAF; Kral, Schroder, Klinke, & Engel, 2003; Lomber et al., 2010). AAF, however, showed somatosensory recruitment in cats deafened within the first month of life (Meredith & Lomber, 2011). Given this high field specificity, we can ask whether such cross-modal takeover fully "preserves" fields from deprivation-induced degenerative changes. The natural assumption would be that fields with reduced functional input show dystrophic changes, including reduced soma size and reduced overall cortical thickness. On the other hand, fields taken over by another function, in this case vision, should exhibit fewer dystrophic changes. Consequently, if cross-modal reorganization was fully 'protective', there should be a dissociation of the effect of deafness between fields that were shown to cross-modally reorganize, such as field DZ (Lomber et al., 2010; Barone et al., 2013; Land et al., 2016), and those where reorganization if this nature was investigated but not observed, such as field A1 (Kral et al., 2003; Lomber et al., 2010). If the same dystrophic changes were to be found similarly in fields with and without cross-modal reorganization, this would indicate that cross-modal takeover is (either in quality or quantity) not sufficient to counterbalance the absence of auditory input.

Here, we analyzed the anatomy of cortical layers in the auditory cortex of CDCs. We investigated three auditory areas: the primary field A1 and the secondary fields DZ and A2. The present study therefore allowed comparison of primary and secondary auditory fields, and between fields that are differentially involved in cross-modal reorganization. Finally, we also investigated visual area 7 as a control field. The study demonstrates general preservation of cytoarchitectonic features in the auditory cortex of deaf cats and a dissociation of the effect of sensory deprivation on cortical layers in both primary and secondary auditory fields, with a reduced layer thickness observed in deep cortical layers but not in supragranular ones.

2 | MATERIALS AND METHODS

This study was performed on eight adult cats. Four of the animals were congenitally deaf and four were of normal hearing. CDCs were selected from the colony of deaf white cats (Kral & Lomber, 2015) using an

early hearing screening procedure described previously (Heid, Hartmann, & Klinke, 1998).

The experiments were approved by the local state authorities and were performed in compliance with the guidelines of the European Community for the care and use of laboratory animals (EU VD 86/609/EEC) and the German Animal Welfare Act (TierSchG).

Additionally to the hearing screening early in life, a hearing test was performed using auditory brainstem responses and confirmed hearing status for all animals before perfusion. For this purpose the animals received 0.25 mg atropine i.p. and were anaesthetized with 15 mg/kg ketamine hydrochloride (Ketamin 10%, WDT, Germany) and 1 mg/kg xylazine hydrochloride (Xylazin 2%, WDT, Germany) applied s.c., with additional doses if necessary over the course of the experiment. The animals' status was monitored using oxygen saturation of capillary blood, capnometry, and electrocardiographic recording. The animals were placed on a homeothermic blanket that ensured a constant rectal temperature of 38°C.

Hearing status was verified using brainstem-evoked responses with condensation clicks applied through a modified DT 48 speaker (Bayer Dynamics, Germany). The speaker membrane was positioned about 1 cm from the tympanic membrane with a custom-made acoustically calibrated sound-delivery device (closed system) inserted into the external auditory meatus after the pinna was removed. Brainstem evoked signals were recorded using an epidural vertex electrode against a reference at the midline of the neck, were preamplified (60 dB, Otoconsult V2 low-impedance amplifier), amplified at a second stage (40 dB, Otoconsult Amplifier-Filter F1, filters 0.010–10 kHz) and recorded using National Instruments MIO cards. The signals were averaged (200 sweeps, repetition rate 33 Hz, Audiology Lab, Otoconsult, Frankfurt am Main). Absence of acoustically evoked brainstem responses (including wave I, generated within the auditory nerve) to 50 μs condensation clicks greater than 110 dB SPL verified profound hearing loss (deafness). In hearing cats, the thresholds were between 5 and 30 dB SPL (Figure 2).

After electrophysiological measurements, the animals were transcardially perfused in deep anaesthesia. Following thoracotomy, 0.5 ml heparin (Heparin Natrium, Ratiopharm, Germany) was injected into the left ventricle and 0.5 ml heparin into the right ventricle. Two liters of 0.9% sodium solution and 2 l fixative (4% paraformaldehyde) and 1 liter of 10% sucrose were then infused transcardially. We monitored the perfusion pressure and maintained it constantly within the range of 120–150 mmHg using a Perfusion One system (Leica Biosystems, Buffalo Grove, IL, USA). The perfusion procedure lasted around 15 min. Subsequently, the soft tissue was removed to allow trephination, the dura mater was opened, followed by an excision of the brain. If required, the brain was postfixated in 4% paraformaldehyde and 10% sucrose overnight. For cryoprotection, each brain was subsequently placed in 30% sucrose solution until it sunk. It was photographed from all directions using a digital camera MC-1260CC/MD (Horn Imaging GmbH, Aalen, Germany), attached to a Zeiss OPMI-1 microscope.

We compared the sulcal pattern around the auditory cortex in the animals investigated (Figure 3). For this purpose, we aligned all brains in the dorsoventral dimension using the dorsal end of the posterior ectosylvian sulcus as a reference point. Subsequently, we aligned the patterns in the rostrocaudal dimension with reference to the intersection of the horizontal line at the level of the dorsal end of the posterior ectosylvian sulcus with the caudal end of the superior sylvian sulcus (Figure 3b). We measured the distance between the caudal and rostral intersection of SSS with this line (an extrapolation of the SSS toward this line proving necessary in one case). The rostrocaudal distance between the posterior and anterior ectosylvian sulcus (determined at the dorsoventral level of the dorsal end of the posterior ectosylvian sulcus) was also measured.

A block of tissue 1.5 × 3.0 cm^2 in size was excised from the brain with great care at the correct cross-sectional orientation in the frontal plane. Additional verification was carried out for this block using the photographs taken before cutting, with additionally correction performed if necessary. The block was frozen at −80°C for 1 hr and cut at −20°C using a Leica cryostat CM3050S (Leica Microsystems GmbH, Wetzlar, Germany) in 50 μm thick sections. We exercised great care in preserving the cutting planes parallel to the frontal plane. Sections were performed in the frontal direction (50 μm, $n = 230–320$) and involved all auditory fields of the cat's brain. Sections were stained subsequently. Every fifth section was stained with SMI-32 and the section thereafter with Nissl. The subsequent three sections were preserved for other purposes.

For SMI-32 immunoreactivity the free-floating sections were demasked in boric acid at 42°C, rinsed three times for 5 min in phosphate-buffered saline (PBS 0.01 M), blocked for 20 min using hydrogen peroxide and rinsed four times for 5 min in PBS. The next step involved blocking the tissue with normal serum to reduce non-specific binding of proteins. Overnight, tissue was incubated with the primary antibody SMI-32 (BioLegend San Diego, CA, USA; Covance Lot: E12EF01151; 1:10,000) at 4°C. Afterwards, sections were rinsed four times for 5 min in PBS, then incubated in secondary antibody with normal serum for 30 min and rinsed three times for 5 min. In the following step, the tissue was exposed to an avidin-biotin-horseradish peroxidase solution (Vectastain Elite ABC, Vector, USA) for 60 min, with subsequent four further rinses of 5 min each. Finally, sections were stained with 3,3′-diaminobenzidine/nickel solution (DAB kit, Vector, USA), given a final rinse, mounted on slides, dried, dehydrated and coverslipped.

The SMI-32 antibody recognizes non-phosphorylated epitopes of the neurofilament protein (Sternberger & Sternberger, 1983), and has previously been used to subdivide the cortex of Old World monkeys (Hof & Morrison, 1995), to parcellate cat visual cortex (van der Gucht, Vandesande, & Arckens, 2001) and to define and distinguish areas of cat auditory cortex (Mellott et al., 2010). SMI-32 visualizes neuronal cell bodies, dendrites and some thick axons in the central and peripheral nervous system (Figure 4). Other cells and tissues are unreactive.

For the Nissl staining, sections were mounted on gelatin-coated microscope slides immediately after cutting, briefly washed with water to remove any residual salts and then stained with cresyl violet (2,5g cresyl violet in 500 ml Na-acetate buffer at pH 3.8–4.0, adjusted with glacial acetic acid) for 14 min. To remove excess stain, tissue was rinsed again with water and ethanol (50%). For dehydration, sections were

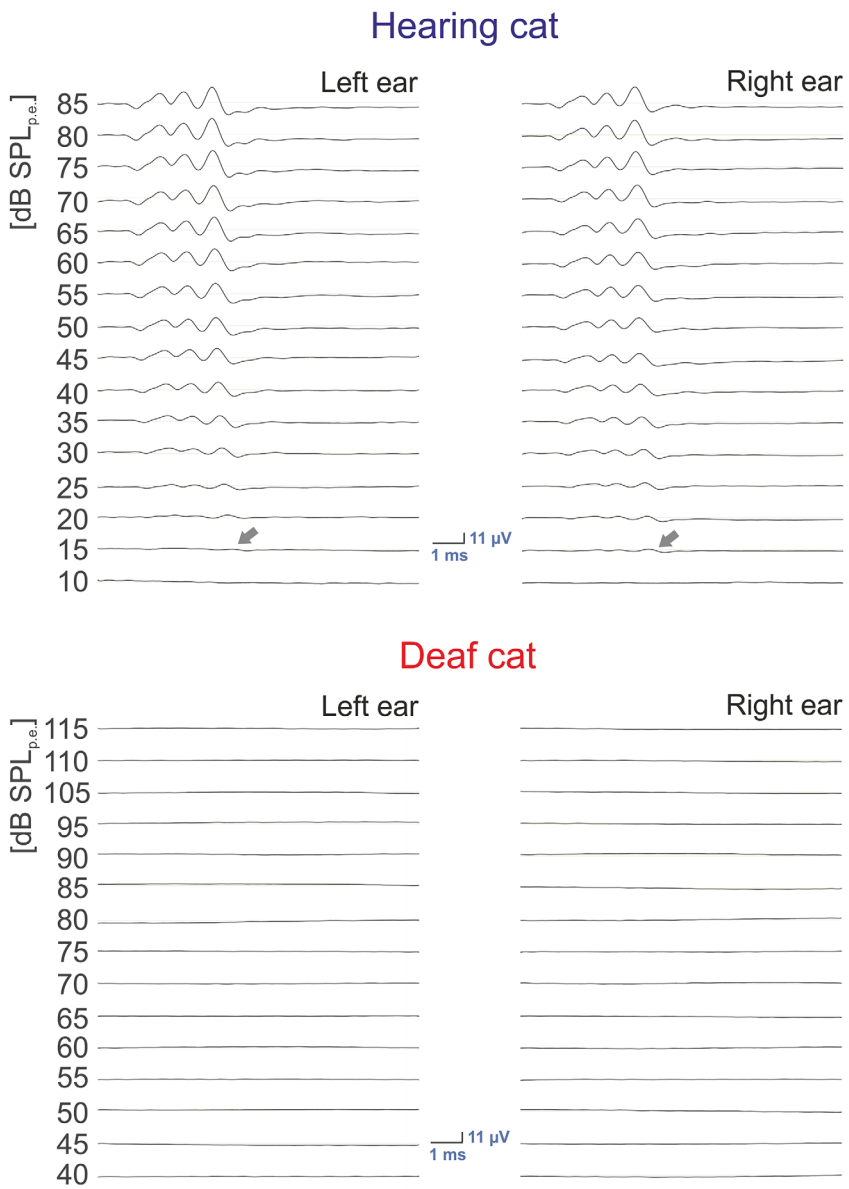

FIGURE 2 Hearing of the animals. Acoustically evoked auditory brainstem responses measured before perfusion in one hearing (top) animal and one congenitally deaf (bottom) animal. In the hearing cat, the typical pattern of brainstem-evoked responses can be observed to appear first at 15 dB SPL_{pe} (arrows), whereas in the deaf cat no discernible responses can be identified up to 115 dB SPL_{pe}. Stimulus: condensation click, 50 µs

washed in ethanol (70% 2 min, 95% 2 min, 100% 2 min, 100% 2 min) and cleared in xylene twice. Finally, sections were coverslipped with Entellan® Neu, Merck, Germany.

The material was subsequently photographed and analyzed with cellSens Dimension software using an Olympus BX45 light microscope and photographed with the Olympus XC30 digital color camera.

In the following, for orientation within the cortical section, vertical direction refers to the direction perpendicular to the cortical surface. Correspondingly, horizontal direction refers to the direction parallel to the cortical surface. Deep layers in the present study refer to layer IV and infragranular layers together.

Six frontal sections were analyzed, three of them being stained using Nissl and three with SMI. These were taken from a stripe in the midpoint of the rostro-caudal extent of A1, as shown in Figure 3. The three sections stained in the same way were separated in rostro-caudal direction by 500 µm, whereas the Nissl and the SMI-32 sections were directly adjacent.

Staining in deaf cats was similar to that previously reported for hearing cats (Figure 4). Firstly, the different auditory fields (AI, A2, and DZ) were localized in each SMI-32 stained section. Areal borders between auditory fields can be identified by the layer-specific differences in density, shape, size, and number of somata and dendrites in SMI-

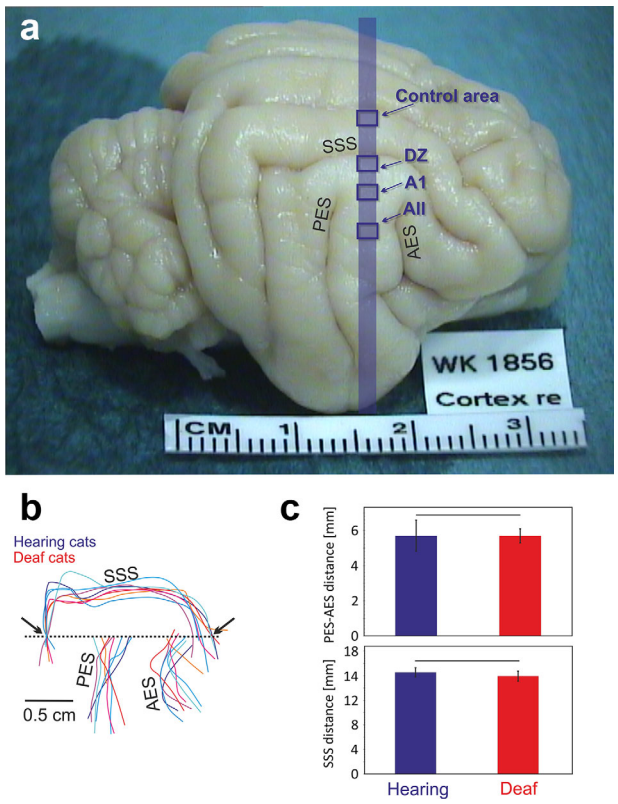

FIGURE 3 Gross anatomy of the auditory brain is not changed in congenital deafness. (a) Brain of a congenitally deaf cat in toto. The blue stripe indicates the position of the evaluated sections: the blue rectangles indicate the position of the investigated cortical areas. (b) Schematic illustration of the sulcal patterns in the auditory cortex normalized in the dorsoventral direction with reference to the dorsal end of the PES (reference point), and in the rostrocaudal direction by the point where the rostrocaudal line crossing the reference point (dashed line) intersects with the caudal portion of the superior sylvian sulcus (arrow). (c) Analysis of the distance between AES and PES (top) and the distance between the caudal and rostral intersections of SSS with the dashed line marked by the arrows (b). All measurements were taken at the level indicated by the dashed line. None of the measures showed significant difference between hearing and congenitally deaf cats ($\alpha = 5\%$, two-tailed Wilcoxon–Mann–Whitney test). AES: anterior ectosylvian sulcus; DZ: dorsal zone; A1: pimary auditory field; AII: secondary auditory field; PES: posterior ectosylvian sulcus; SSS: superior sylvian sulcus

32 staining (Figures 4–5; Mellott et al., 2010). These boundaries are, however, transitional and a transition zone is difficult to assign to any of the regions. All subsequent measurements were therefore taken outside of these transitional zones (arrows in Figure 5b). AI is located in the dorsal half of the middle ectosylvian gyrus, while the secondary auditory cortex (A2) is positioned at the ventral border of AI, between the anterior and superior ectosylvian sulci (Reale & Imig, 1980). The DZ is located dorsal to AI (He & Hashikawa, 1998).

SMI-32 preferentially labels layers III and V, both of which appear as dark bands (Mellott et al., 2010). A greater number of stained pyramidal neurons and heavy neurophil labeling are characteristic of layer V in A2 as compared with AI (Winer, 1992; Mellott et al., 2010). In layers III and V of DZ a higher number of somata and dendrites and denser reactivity of somata helps to distinguish this area from AI (Mellott et al., 2010). The thickness of the cortex layers (I/II, III, IV, V, VI) was measured at five different positions per section, throughout each area. The layer borders were quite clearly identifiable since we had a 50 μm thick section that allowed focusing through the section (in the *z* direction). Using this approach, including regions where the staining was sparse (such as field A1), allowed the field boundaries and the borders of cortical layers to be identified with confidence.

An area (designated as area 7) within the same section that had laminar staining patterns similar to those of the auditory areas was used for comparison. Area 7 receives main inputs from the secondary visual areas 19, 20, and 21 (Symonds & Rosenquist, 1984) and is located in the crown of the middle suprasylvian gyrus between area 19 and posterior medial-lateral suprasylvian visual area (posterior MLS, Palmer, Rosenquist, & Tusa, 1978). This area was particularly suitable, exhibiting distinct spatial separation from auditory areas and yet having a similar cytoarchitecture (staining pattern), enabling the same layers to be directly evaluated and compared (which would have been difficult for areas 17, 18, and 19, as these have a particular, distinct lamination in the cat; see Figure 5). In area 7, layers III and V show a lower density of neurons and are less stained than in adjacent visual fields. The immunopositive dendrites penetrating the other layers are less dense and stained only moderately; this additionally helps to distinguish area 7 from surrounding visual areas (van der Gucht et al., 2001).

For measurements in those sections stained with cresyl violet, not all layer borders could be determined (Figure 4a). The auditory supragranular layers have a more uniform appearance than other areas of the cortex and borders are particularly difficult to identify. Layer IV has almost no pyramidal neurons (Winer, 1992), while they are abundant in layer III, especially in the latter's deeper half (Winer, 1984a,b). Furthermore, while there is some blurring of lamination in Nissl-stained sections within layers II and III, layer IV tends to be less dense than the supragranular layers. It therefore proved possible to reliably determine the border between layer III and layer IV using Nissl staining. The position was verified further and double-checked for each section by comparison with the adjacent SMI-32 section, where this border was also well discernible. The determination of the areal borders and identification of the area where the measurements were taken was derived from the adjacent SMI-32 staining, where areal borders could be better observed.

Differences in immunoreactivity were used to measure the thickness of the individual layers in the SMI-32 stained sections. Layers I and IV have no immunoactive neurons, whereas layers II and VI show weak to moderate immunoreactivity and layers III and V the highest immunoreactivity (Mellott et al., 2010). Because it was not possible to distinguish the border between layers I and II in all sections, they were considered together. Layer VI was very hard to isolate from the white matter, since the stain was fading in the direction of the white matter without any distinct border. We therefore excluded layer VI from analysis in the SMI-32 staining.

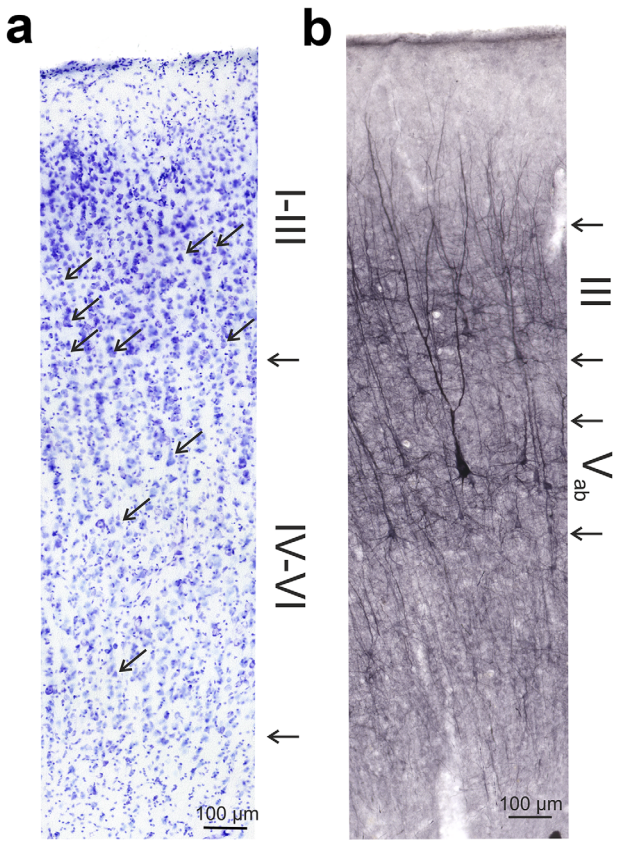

FIGURE 4 Detail of the staining in a hearing control. (a) Nissl staining marks cells throughout the whole auditory cortex and reveals some aspects of cortical cytoarchitecture. Arrows in the image point to examples of pyramidal cells that are present in supragranular layers but not in layer IV; the arrows on the side point to the border of layer III and IV and the boundary between layer VI and white matter. (b) SMI-32 stains somata and dendritic trees and reveals the dendritic anatomy in detail. The method stains cells in layer III and V. The cells are well differentiated from the background and indicate the cortical layer they are located in. The arrows on the side mark the borders of layer III and V_{ab} as used in the present study to quantify layer thickness

The border between layers II and III was identified based on the appearance of densely labeled pyramidal cell somata (Figure 4b). Their most superficial components constituted the outer boundary of layer III. Additionally, the inner border of layer III was characterized by the disappearance of the cell somata. Finally, layer V was determined in a similar manner, based on the appearance and disappearance of the somata of well-stained large pyramidal neurons. Layer V can be divided into three subparts (V_a, V_b, and V_c) (Kelly & Wong, 1981; Winer & Prieto, 2001). Layers V_a and V_b contain pyramidal cells, whereas layer V_c is usually devoid of pyramidal cells. Given that the somata of pyramidal cells were used for delineation of laminar borders in this study, the results for layer V probably include only sublayers V_a and V_b.

Layer thickness was assessed at five different places distributed as equidistantly as possible within a given area in the particular section. Measurement was performed in the perpendicular direction to the cortical surface at a given position, using the Olympus Cell Sense Software package that allowed the distance between two spots within the section to be determined.

2.1 | Statistical Analysis

The data were statistically compared using the Wilcoxon–Mann–Whitney test (two-tailed, $\alpha = 5\%$). Since measurements were taken five times in the same section, the probabilities were Bonferoni-corrected to account for the multiple comparisons. We further normalized the results relative to the data obtained in the area 7. (This area was suitable for normalization purposes as it is located in the same section, close to the areas evaluated and has the same layers stained.) To achieve normalization, a mean was computed from the five measurements taken in each area. The means obtained in for the field of interest were subsequently divided by the means for the control field. Normalized thickness values of greater than 1 thus indicate thicker auditory areas than area 7, those less than 1 indicating thinner auditory areas. These data again underwent statistical comparison using the Wilcoxon–Mann–Whitney test (two-tailed, $\alpha = 5\%$); the probabilities were used uncorrected. For control area 7, the medians ($\pm$ absolute deviation) are in some cases compared in the text.

3 | RESULTS

Firstly, we compared acoustically-evoked brainstem responses obtained at the beginning of the experiments (Figure 2). All hearing cats had brainstem-evoked response thresholds between 5 and 30 dB SPL_{pe}. All CDCs had non-detectable brainstem responses up to the level of 115 dB SPL_{pe}, demonstrating a difference of $\geq$90 dB, and thus profound hearing loss (deafness). The result in all CDCs was consistent with the outcome of hearing screening outcome performed at 4 weeks post natally (Heid et al., 1998).

The two groups of animals did not differ in age at experiment (hearing: 4.2 ± 3.2 years; CDCs: 4.1 ± 0.9 years, two-tailed Wilcoxon–Mann–Whitney test, $p = 0.94$) or in weight (hearing: 4.1 ± 1.3 kg, CDCs: 3.6 ± 0.7 kg, two-tailed Wilcoxon–Mann–Whitney test, $p = 0.54$). We additionally compared the sulcal pattern surrounding the auditory cortex in the investigated animals (Figure 3b,c). None of the measured intersulcus distances showed significant differences between the two groups (Figure 3c).

Next, we analyzed the sections (Figure 4). In hearing controls, the pattern of staining using Nissl and SMI-32 corresponded to that in previous studies (Figure 4). With SMI staining in the present study, we observed subtle, sparse staining of neurons in layer VI (field A1), both in hearing and in CDCs (Figure 5c, marked by the arrow in A1 panel). This has not been noted previously.

In general, the cytoarchitectonics in CDCs was not obviously different from the hearing controls (Figure 5). We were able, to a similar extent in both groups of animals, to identify both the typical microcolumns using Nissl staining as well as the typical layering associated with both Nissl and SMI-32 staining. The size, density, and laminar distribution of SMI-32 neurons differed across neocortical fields (Campbell & Morrison, 1989). Using the same cytoarchitectonic criteria

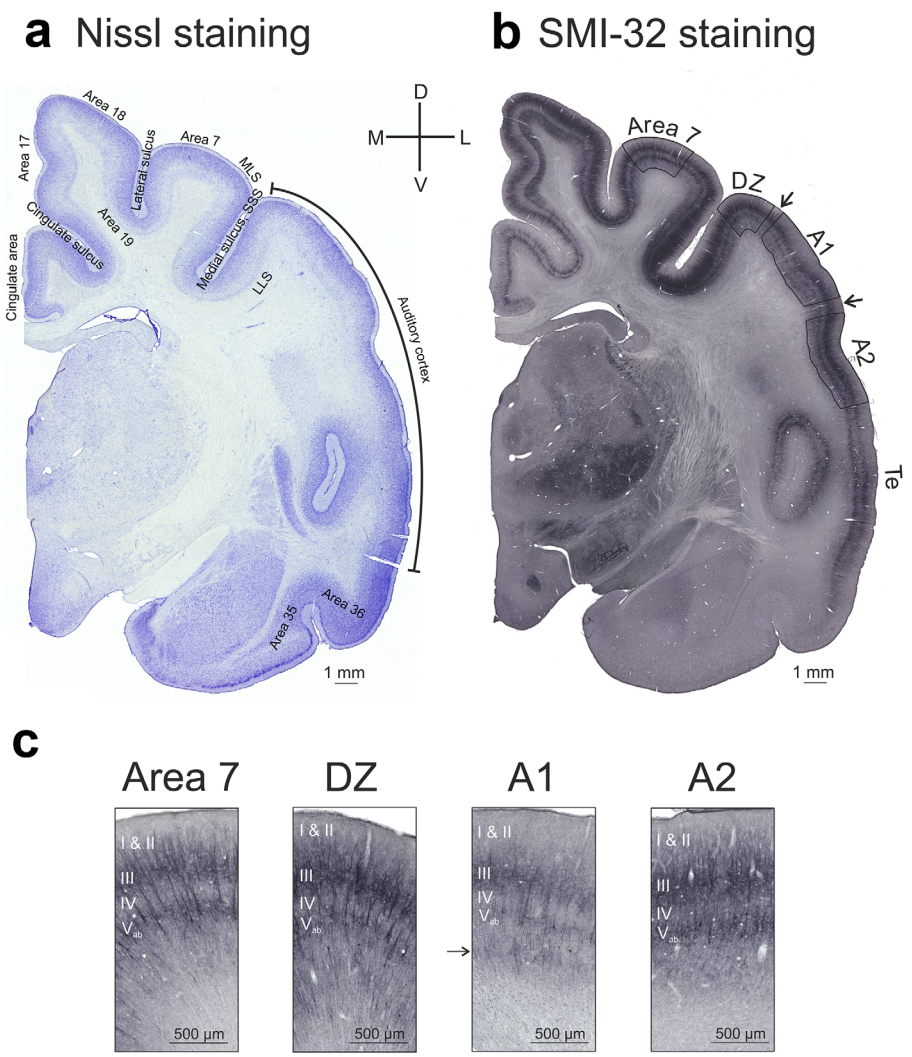

FIGURE 5 Cytoarchitecture in the CDCs is preserved despite absence of hearing. Shown are sections (whole hemispheres) with (a) Nissl staining and (b) SMI-32 antibody staining. The sections show a generally preserved cytoarchitectonic patterns in the deaf cat. It proved possible to reliably delineate all areas investigated using these staining techniques. Note that area Te runs close to the sulcus; due to tangential section, this area could not be evaluated. (c) Details of all four investigated areas in the congenitally deaf cat with the typical differences in staining intensity and pattern using SMI-32 antibody staining. Arrow points to the stripe of darker staining in layer VI that has not been previously described in A1 of hearing cats and was observed here in both hearing and deaf cats. MLS: medial-lateral suprasylvian area

(Mellott et al., 2010), we were able to identify all investigated cortical fields and cortical layers both in the auditory cortex and in the other cortical regions of CDCs (Figure 5). The borders of area 7 were less clearly delineated in many sections, particularly its boundary to the medial part of the lateral suprasylvian sulcus regions (AMLS and PMLS). In order to safely remain within area 7, we performed all measurements in the dorsomedial half of the suprasylvian gyrus (Figure 5). In subsequent measurements we avoided transition zones between auditory fields.

We first analyzed the cortical thickness in Nissl-stained sections. In general, the cortical area 7 (summed up data from all layers) was never thicker than the auditory cortex; this applied to both hearing and deaf animals. With the exception of DZ in hearing cats, it was thinner than the auditory fields (data not shown, two-tailed Wilcoxon–Mann–Whitney test, $\alpha = 5\%$). This was frequently evident from visual inspection at low magnification. In Nissl-stained sections, the border between layer III and layer IV and the border of the white matter were distinguished with confidence (Figure 4a). Consequently, in Nissl-staining, we analyzed the overall thickness of the cortex and additionally the thickness of supragranular layers (layer I–III) and deep layers (layer IV–VI; Figure 4). The CDCs had thinner cortices than hearing cats in fields A1 and A2, but not in DZ and area 7 (Figure 6). The differences were small (~200 µm) but significant. All differences were caused by the deep layers (Figure 6c). In all of these measurements, the control area 7 of CDCs was not significantly different from the hearing controls. These data suggest a modality-specific dystrophic change in deep layers of the auditory cortex in CDCs. The situation for area DZ was less clear-cut, since here the supragranular layers had a tendency towards slightly more variance and greater thickness in CDCs. This may be related to the location of DZ in the crown of a gyrus and thus the curvature of the cortex.

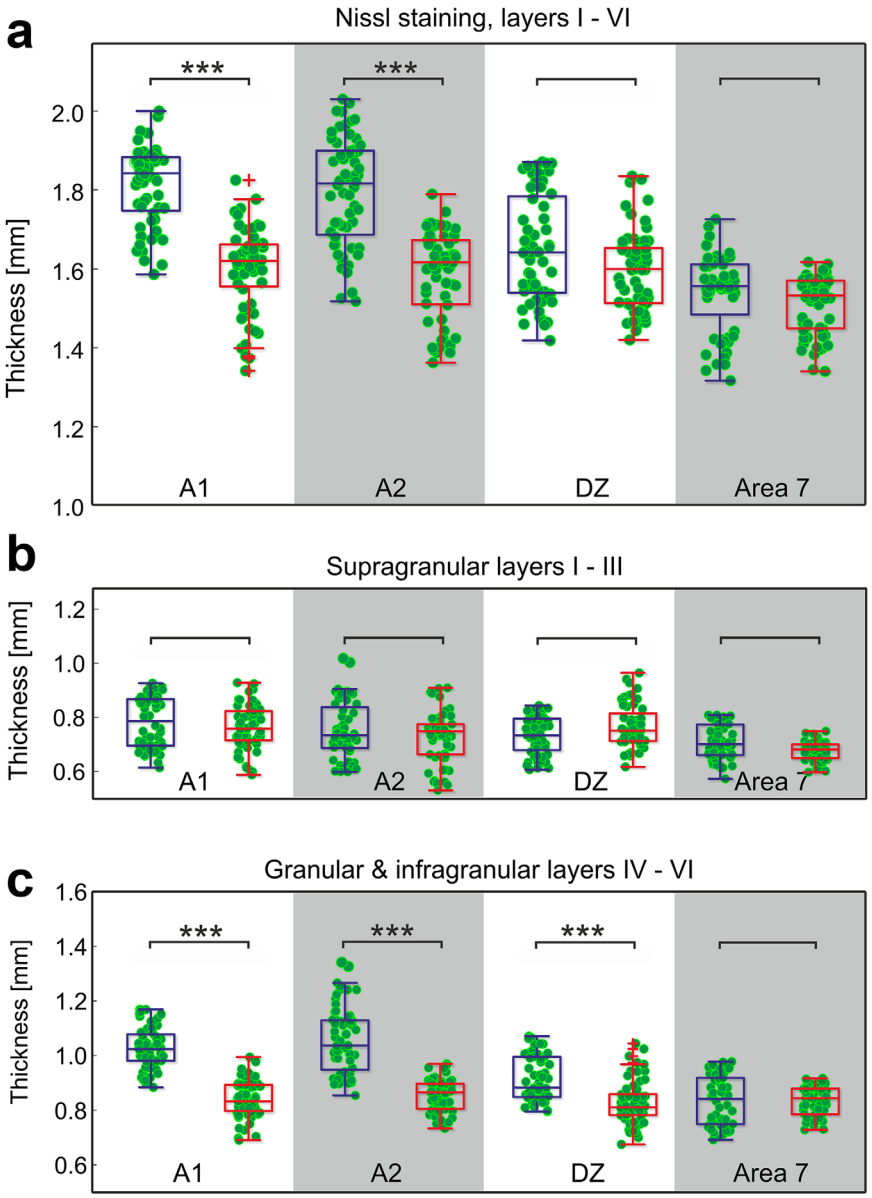

FIGURE 6 Nissl staining reveals reduced thickness of deep layers in deaf cats. (a) Overall cortical thickness is reduced in A1 ($p = 3.7*10^{-15}$, Bonferroni-corrected two-tailed Wilcoxon–Mann–Whitney test) and A2 ($p = 8.5*10^{-12}$), but not in DZ ($p = 0.4$) and area 7 ($p = 0.1$). (b) No change in layer thickness of supragranular layers (layers I–III, $\alpha = 5\%$). (c) The deficit is entirely due to reduced deep layers (layers IV, V, and VI; A1: $p = 1.31*10^{-18}$; A2: $p = 3.99*10^{-17}$; DZ: $p = 9.05*10^{-8}$; area 7: $p = 0.11$). Blue: hearing cats; red: congenital deaf cats. *** $\sim p < 0.001$

The second step involved analysis of cortical layering in SMI-32 sections. As with Nissl staining, in SMI-32 none of the comparisons revealed the control region to be different between the two groups of animals (two-tailed Wilcoxon–Mann–Whitney test, $\alpha = 5\%$).

Since layers I and II could not be reliably differentiated, we considered them together. In all areas investigated the thickness of these layers did not differ between the two experimental groups (Figure 7a; in area 7: hearing animals: 404 ± 44.0 μm; CDCs: 404 ± 9.4 μm; $p = 0.48$, corrected). We subsequently analyzed the data relative to the control area, dividing the means of all five measurements in the auditory region of a given section by the mean value obtained in the control region for the same section. This reduced the amount of data by a factor of five, but allowed a relation between an auditory and a non-auditory area in the same section to be considered. In the normalized data, too, there was no obvious difference between the two groups (Figure 7b). The population medians had the tendency to exceed 1, thus layer I and II of the auditory cortex were often thicker than those of the control area for the same section.

Layer III was reliably identified in the SMI-32 sections. This layer did not differ between the two groups either in the absolute or relative thickness (Figure 8; data for area 7: hearing animals: 286.2 ± 27.9 μm; CDCs: 273.0 ± 12.5 μm, $p = 0.205$, corrected). Layer III of the auditory cortex was about 10% thicker than the control area for the same section. It is notable that the range of values observed, particularly the normalized range, was smaller in CDCs.

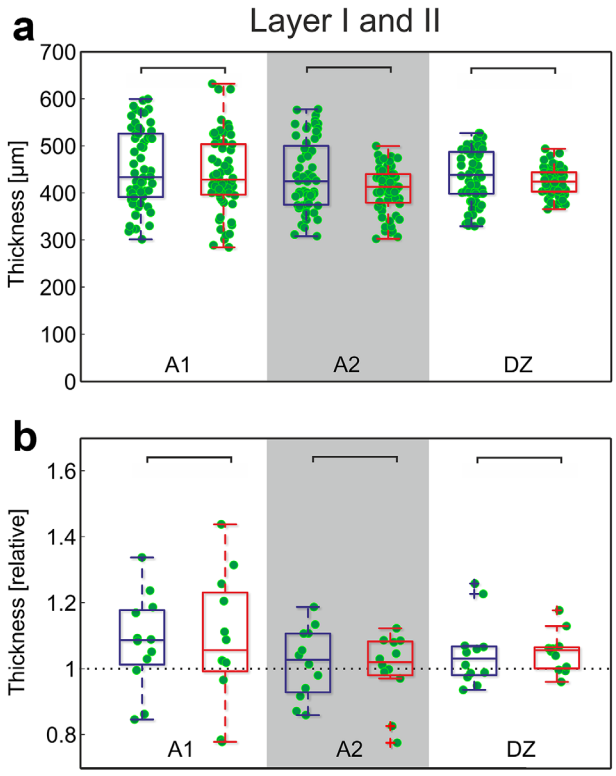

FIGURE 7 SMI-32 staining reveals no effects of deafness on thickness of layers I + II. (a) Direct comparison of the measurements in absolute data ($\alpha = 5\%$, Bonferroni-corrected two-tailed Wilcoxon–Mann–Whitney test). (b) Normalized results. Mean data from each section in auditory cortex were divided by the corresponding mean result in area 7. No difference observable in normalized results ($\alpha = 5\%$, uncorrected). Blue: hearing cats; red: congenital deaf cats

Layer IV was differentiated in the SMI-32 sections by exclusion: both the border of layer III and the upper border of layer V were reliably identified, and, consequently, the region in between (mostly devoid of stained cells) was layer IV. Here, a difference emerged in all auditory areas (apart from control area 7: hearing animals: 153.4 ± 6.0 µm; CDCs: 147.4 ± 9.5 µm; $p = 0.080$, corrected): layer IV was slightly but significantly thicker in hearing cats (Figure 9). The difference was also well discernible in the normalized plot, in which nearly all mean values for hearing cats exceeded 1, whereas more than 50% of the CDCs had values below 1.

Layer V (as determined here) was thinner than described in the literature (350 µm, Winer & Prieto, 2001); we assume that what has been analyzed here is only a portion of layer V. It is the deeper part of layer V, the sublayer V_b that is characterized by sparsely distributed large pyramidal neurons and, using Nissl staining, typically appears as a "light band" with occasionally very large neurons; it is around 200 µm thick (Winer & Prieto, 2001; Rose, 1949). Winer and Prieto additionally identify a small pyramidal cell containing sublayer V_a (75 µm) and a third thin sublayer V_c with small nonpyramidal cells (75 µm). Given the thickness and the large pyramidal neurons stained with SMI-32 we have likely identified sublayers V_b and partly V_a (containing pyramidal cells) but may have missed sublayer V_c. We designated the boundaries of this layer as V_{ab} to make clear that the thickness does not reflect the layer V in its entirety.

Layer V_{ab} was significantly thinner in deaf cats for all auditory areas (Figure 10). Control area 7 was not significantly different (hearing animals: 195.3 ± 18.6 µm; deaf: 201.9 ± 8.0 µm; $p = 0.19$, corrected). Of particular interest were the differences in the normalized data (Figure 10), where they appeared to be nearly categorical: while all data for hearing animals were greater than 1, nearly all those from CDCs were less than 1. This further documents that the decrease in thickness of the deep layers in CDCs is not due to size or staining differences between sections.

4 | DISCUSSION

We analyzed the cytoarchitectonic pattern of the neocortex in adult hearing and CDCs. There was no obvious difference in the general pattern of staining between deaf and hearing animals within auditory or non-auditory regions. This documents that the general pattern of cortical cytoarchitectonics is not dependent on sensory input, even if absent from birth and persisting for about 4 years.

The present data, however, demonstrate a small but significant reduction in thickness of layer IV and the infragranular layers for

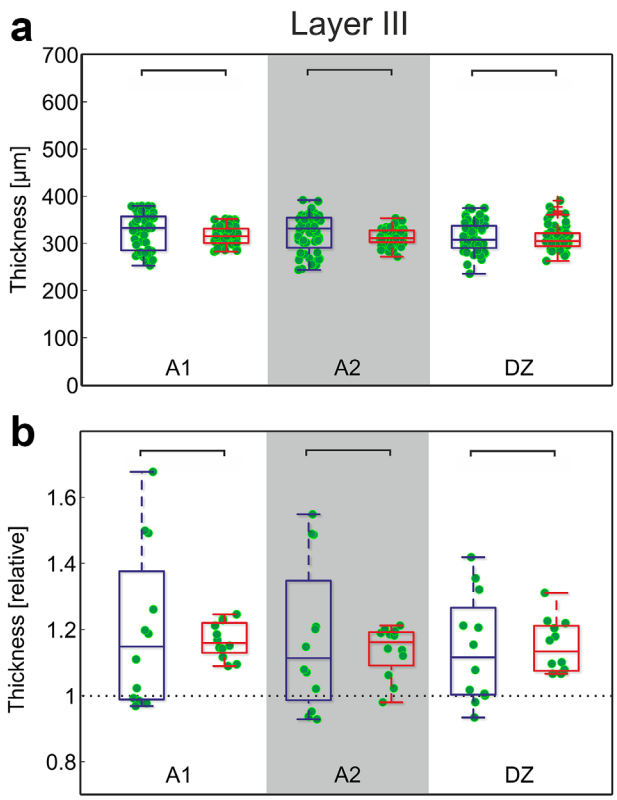

FIGURE 8 SMI-32 reveals no effect of deafness on thickness of layer III. (a) Direct comparison of the measurements in absolute data ($\alpha = 5\%$, Bonferroni-corrected two-tailed Wilcoxon–Mann–Whitney test). (b) Normalized results. Mean data from each section in auditory cortex were divided by the corresponding mean result in area 7. No difference observable in normalized results ($\alpha = 5\%$, uncorrected). Blue: hearing cats; red: congenitally deaf cats

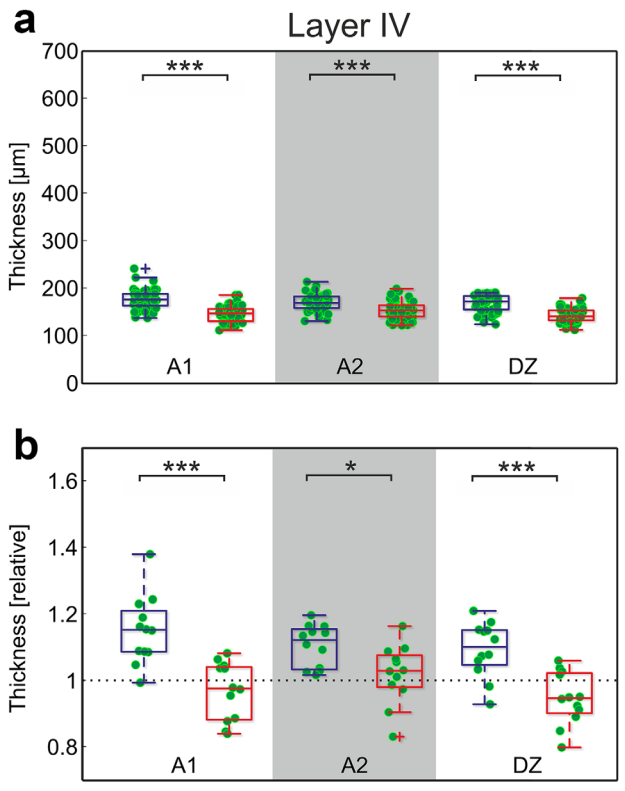

FIGURE 9 SMI-32 reveals thinner layer IV in deaf animals. (a) Direct comparison of the measurements in absolute data between hearing and deaf cats (A1: $p = 6.01*10^{-13}$; A2: $p = 1.42*10^{-5}$; DZ: $p = 3.44*10^{-11}$; Bonferroni-corrected two-tailed Wilcoxon–Mann–Whitney test). (b) Normalized results. Mean data from each section in auditory cortex were divided by the corresponding mean result in area 7. In hearing controls, the auditory cortex layer IV is thicker than area 7; in deaf animals, this is not observable (comparison hearing vs. deaf cats, A1: $p = 0.00019$; A2: $p = 0.022$; DZ: $p = 0.00073$, uncorrected). Blue: hearing cats; red: congenital deaf cats. *** $\sim p < 0.001$; * $\sim p < 0.05$

several auditory fields in animals with congenital deafness. This applies to both absolute and relative measures. The effect was not observed in the visual field (area 7) that served as a control and a reference for normalization. While this does not rule out deprivation-induced morphological changes in supragranular layers, the study shows that layer IV and infragranular layers are more susceptible to effects of deprivation than supragranular layers. Finally, and for the first time, this study demonstrates deprivation-induced dystrophic changes beyond the primary auditory cortex (in both investigated fields DZ and A2).

The overall loss of around 200 µm documented for layers IV–VI using Nissl staining was greater than the thickness lost (~100 µm) in layers IV and V_{ab} in SMI-32 staining. It is, therefore, likely that layer VI (which could not be evaluated in SMI-32) also contributes to the thinner deep layers in Nissl staining.

4.1 | Discussion of methods

The present investigation referred to the criteria for areal cytoarchitectonics in SMI-32 as suggested by Mellott et al. (2010). Use of these criteria enabled the areas to be differentiated reliably in all animals. Furthermore, while staining was variable between individual animals, we did not observe a systematic difference in staining quality between hearing and deaf animals. This is important, since it demonstrates that areal cytoarchitecture is not extensively affected by developmental experience (see Figure 5 for a congenitally deaf animal).

The layer-specific differences between hearing and deaf cats observed here were not apparent from direct visual inspection—they required detailed quantitative analysis under precisely defined criteria. The key factors in detecting these subtle differences are 3-fold:

1. We were careful to avoid sections at the proximity of sulci that are likely to include tangentially cut cortex from the curvature of the sulcus. Tangential sections make the cortex appear thicker than it actually is. Such sections can be identified (1) by the presence of cells and vessels that are sectioned perpendicularly or obliquely and (2) because a majority of neuronal somata have 'cut-off' apical dendrites or absent dendritic trees. Since sections were partly tangential in area Te, we excluded the latter from the present analysis.

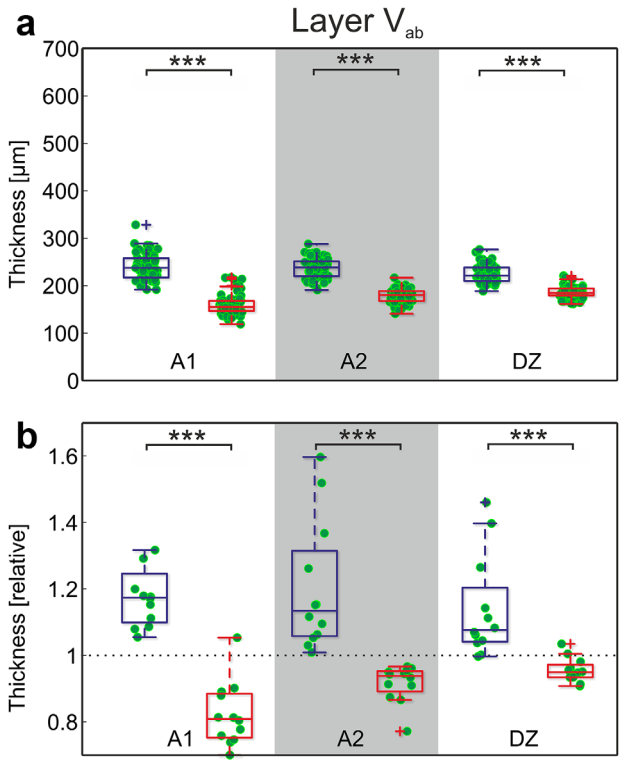

FIGURE 10 SMI-32 reveals thinner layer V_a+V_b in deaf animals. (a) Direct comparison of the measurements in absolute data (A1: $p = 3.59*10^{-19}$; A2: $p = 8.71*10^{-20}$; DZ: $p = 2.44*10^{-13}$; Bonferroni-corrected two-tailed Wilcoxon–Mann–Whitney test). (b) Normalized results. Mean data from each section in auditory cortex were divided by the corresponding mean result in area 7. In hearing controls, the auditory cortex layer V_{ab} is thicker than area 7; in deaf animals, the auditory cortex is thinner (A1: $p = 3.66*10^{-5}$; A2: $p = 3.66*10^{-5}$; DZ: $p = 9.73*10^{-5}$; uncorrected). Blue: hearing cats; red: congenital deaf cats. *** $\sim p < 0.001$

2. We maintained perfusion pressures above 120 mmHg and perfused in a rather short period of time with additional use of 10% sucrose. Shrinkage of brain tissue is about 3% using this procedure (data from electrode penetration reconstructions in Land et al., 2016, compared with 11% in our previous studies; see appendix in Kral et al., 2000). Variable (and considerable) shrinkage may obscure small effects on layer thickness.
3. The precision of the sectioning plane is another key issue; this is particularly difficult to ensure in large brains and in areas distributed over large regions.

Confounding factors are unlikely to have influenced the present results, since there was a dissociation of the effect with respect to the layer (no effect in supragranular layers, but an effect in deep layers) and dissociation with respect to area: auditory areas exhibited this effect, but control area 7 from the same sections did not. Finally, we used two different staining methods that generated consistent results where comparable. Thus, the results are not specific to a staining method or to a particular means of processing the sections for staining purposes.

5.2 | Discussion of results

The finding of thinner deep layers in the auditory cortex of CDCs is consistent with previous functional studies demonstrating reduced responsiveness in infragranular layers of deaf cats when stimulated with cochlear implants (Kral et al., 2000, 2006b). Chronic electrostimulation with cochlear implants initiated early in life was able to reverse this effect (Klinke, Kral, Heid, Tillein, & Hartmann, 1999; Kral, Hartmann, & Klinke, 2006b). Consequently, it is the loss of auditory input that is responsible for the reduced activity. Previous reports of a delay in synaptogenesis and pronounced synaptic pruning in primary fields are highly consistent between blind and deaf animals (anatomy, visual system: Cragg, 1975a,b; Winfield, 1981, 1983; function, auditory system: Kral et al., 2005; review: Kral & Sharma, 2012) and point to a developmental cortical sequence that is highly dependent on experience.

The present outcomes are in line with human literature demonstrating reduced white matter volume (Hribar, Suput, Carvalho, Battelino, & Vovk, 2014), correspondingly reduced myelination in the auditory cortex of congenitally deaf humans (Emmorey, Allen, Bruss, Schenker, & Damasio, 2003), and reduced cortical thickness in different regions of the brain of congenitally deaf humans (Li et al., 2012). However, the extent of changes observed here is probably below the resolution of human imaging. Changes in areal size were not the focus of the present study. The analysis of sulcal patterns (Figure 3b,c) was used only to rule out larger differences in brain gross anatomy. A previous study described slight shifts in areal borders in cats deafened at the end of the first month of life (Wong, Chabot, Kok, & Lomber, 2013).

The present study alone cannot clarify which structure (neuronal somata or the neuropil) became smaller in CDCs. In the auditory pathway, there are indications that both are involved in dystrophic changes. In the brainstem of CDCs, reduction in soma size by about 30% has been reported throughout the auditory nuclei (Saada et al., 1996; Heid, 1998), demonstrating the trophic influence of auditory activity in auditory structures. Similar findings exist for neonatally deafened animals (Hultcrantz et al., 1991; Stakhovskaya, Hradek, Snyder, & Leake, 2008). However, there is also indication of smaller dendritic trees in neurons of the auditory cortex of CDCs (Kral, Hartmann, & Klinke, 2006a) and a similar effect after hearing loss in the rabbit (McMullen & Glaser, 1988; McMullen, Goldberger, Suter, & Glaser, 1988). Reduced synaptic counts have been morphologically demonstrated in the midbrain of deafened cats (Hardie et al., 1998) and functionally in the cortex of CDCs (Kral et al., 2000). Since neither of the staining methods used in the present study delineates the border of the cells, cell size could not be investigated directly. However, it is likely that a combination of factors—dystrophic reduction of cell soma, smaller dendritic trees, reduced myelination and reduced number, and size of synaptic spines—contribute to the present observation.

The outcomes of the present study go beyond previous functional observations (Kral, Tillein, Heid, Klinke, & Hartmann, 2006b) by demonstrating that the deficit in infragranular layers also has a morphological correlate. Furthermore, the present study shows that areas beyond the primary auditory cortex undergo similar dystrophic changes. It also demonstrates the involvement of layer IV in these dystrophic changes. Layer IV generates only weak current source density signals (Kral et al., 2006b) and therefore the functional correlates in previous studies might have been beneath the detection threshold.

The results point to a developmental difference in the effects of deafness on various layers, but they provide no clear explanation as to why deep layers should show more dystrophic changes than supragranular layers. While supragranular layers represent a structure that processes bottom-up sensory input, the infragranular layers represent the executive output of cortical columns projecting not only into the auditory thalamic nuclei, but also to the auditory midbrain and even other brainstem structures (Mellott, Bickford, & Schofield, 2014; Schofield, 2009; Znamenskiy & Zador, 2013). One possible function of infragranular layers is the control of plasticity in the subcortical auditory pathway by efferent projections (Suga & Ma, 2003; Bajo, Nodal, Moore, & King, 2010; Xiong et al., 2015). The existence of wide-ranging dystrophic changes in deaf or deafened animals in the cochlear nucleus and inferior colliculus (see above), and the present data from the auditory cortex may be associated with reduced neuronal activity in these structures. In congenital deafness, the evidence for cross-modal recruitment within the lemniscal pathway is very limited. In the absence of such cross-modal change and in absence of auditory input, control of subcortical activity via efferent loops has no effect on cortical input and is therefore likely never functional. This may also relate to non-auditory projection of deep layers and explain these findings.

In addition to dystrophic changes in field A1, there was a corresponding change in the secondary auditory fields. This is interesting, since additionally to projection to different subcortical targets (Reale & Imig, 1983; Alvarado, Stanford, Rowland, Vaughan, & Stein, 2009; Chabot, Mellott, Hall, Tichenoff, & Lomber, 2013) they are also sources of feedback projections into A1. Such feedback projections

from infragranular layers either target infragranular layers at a lower hierarchical level or, in case of higher hierarchical separation, layer I (Markov et al., 2014; de la Mothe, Blumell, Kajikawa, & Hackett, 2006). Furthermore, there is a short-distance feedback projection within the supragranular layers (reviews in Markov et al., 2014; de la Mothe et al., 2006). The present observation of dystrophic changes in infragranular layers are likely associated with feedback projections arising from infragranular layers being less active in congenital deafness.

5.2.1 | Visual cross-modal reorganization did not prevent dystrophy in "deaf" area DZ

Higher-order auditory areas are recruited by visual stimulation in congenital deafness (Naito et al., 1997, 2000; Nishimura et al., 1999; Petitto et al., 2000; Finney, Fine, & Dobkins, 2001; Finney, Clementz, Hickok, & Dobkins, 2003; Lomber et al., 2010; Leonard et al., 2012). Robust auditory responsiveness in secondary auditory area DZ of CDCs has been demonstrated recently despite cross-modal (visual) take-over of a scattered neuronal population in this field (Land et al., 2016). The present findings complement these results by showing that the dystrophic effect of congenital auditory deprivation is widespread and cross-modal take-over of field DZ does not fully preserve the anatomical structure of layers IV–VI in this field.

5.2.2 | Specificity of the changes to auditory cortex and infragranular layers

It is interesting that the dystrophic effect was not observed in supragranular layers. The effect cannot be only due to loss of activity in the thalamocortical projections. Layer IV receives the strongest thalamocortical input. However, while the most abundant terminals from thalamic neurons are in layer III, all layers receive some thalamic inputs (Mitani & Shimokouchi, 1985; Mitani et al., 1985; Winer & Lee, 2007). In fact, thalamic input, while not functionally active, is anatomically preserved in both A1 and DZ of CDCs (Barone et al., 2013); in A1 it has a preserved cochleotopic arrangement despite smearing (Barone et al., 2013). Furthermore, thalamic input is functional both in A1 and in DZ if auditory nerve is electrically stimulated in CDCs (Hartmann et al., 1997; Land et al., 2016).

The present study provides evidence that adaptation to deafness differs between upper and deep layers. To allow the differential dystrophic effects between these layers, the coupling of supragranular to infragranular layers must be abnormal in congenital deafness. The supragranular layers are mutually interconnected by short-distance lateral connections between neighboring columns, by feedforward connections between areas and short-distance feedback connections between areas (Figure 11a, Markov et al., 2014). The infragranular layers are connected by short-distance feedforward connections and long-distance feedback connections between areas (for review, see Markov et al., 2014). Thus, there are mutual connections within both the superficial, and the deep layers. The main connection between supra- and infragranular layers is within columns (Figure 11a): normally, supragranular layers activate deep layers by means of a direct intracolumnar connection (review in Raizada & Grossberg, 2003; Douglas & Martin, 2004; Harris & Mrsic-Flogel, 2013; Jiang et al., 2015).

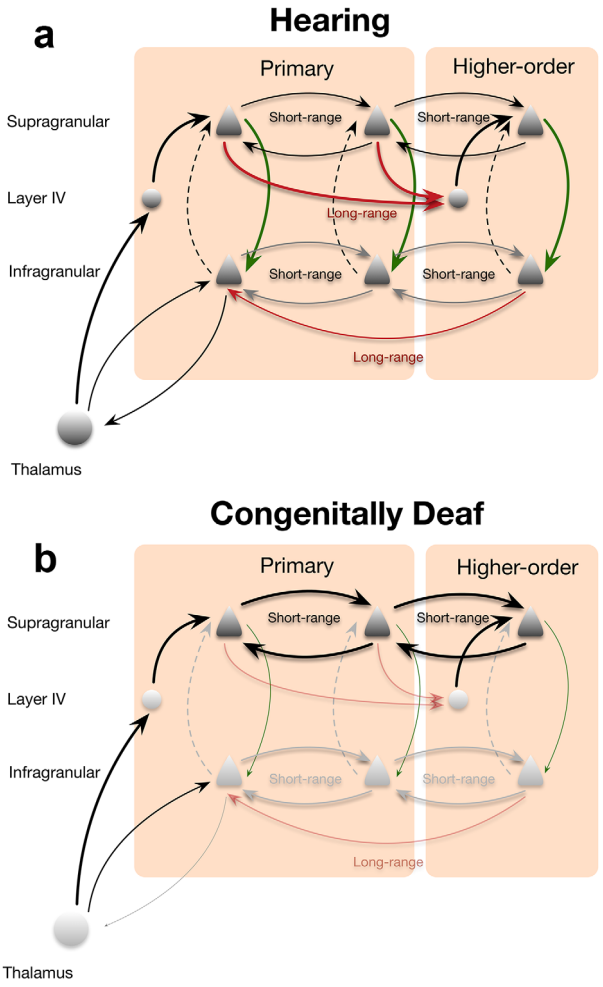

FIGURE 11 Schematic illustration of the effect of congenital deafness on cortical columns. (a) Schematic illustration of connectivity between layers and areas in hearing animals. Green arrow marks the driving connection between supragranular and infragranular layers, dashed lines indicate modulatory effect of the connection from infragranular to supragranular layers. (b) In congenitally deaf cats, the intracolumnar connection from supragranular and infragranular layers (green) and long-distance connections between cortical areas are weakened and short-range connectivity in supragranular layers is strengthened

Previously, based on current source density profiles evoked by electric stimulation in CDCs, it has been suggested that this supra-to-infragranular layer projection is weakened in congenital deafness (Kral et al., 2000). This is likely to be a factor involved in the present findings. Since the anatomical supra-to-infragranular projection develops early during development (Burkhalter, Bernardo, & Charles, 1993), weakening of this connection is probably functional and not anatomical (Figure 11b). Interestingly, with focused intracortical microstimulation of supragranular layers in the primary auditory cortex, infragranular layers could not be recruited in normal-hearing guinea pigs (Voigt, Hubka, & Kral, 2017). Similarly, in a brain slice from rat barrel cortex, stimulation of supragranular layers was not capable of activating infragranular layers (Constantinople & Bruno, 2013). In combination, this indicates that the

connection from supragranular to infragranular layers cannot be recruited by stimulation of supragranular layers alone: either the thalamic input to infragranular layers or a corticocortical top-down input to these layers (Larkum et al., 2004) is additionally required to provide sufficient drive to activate deep layer neurons above firing threshold.

The reverse projection, from infragranular layers into supragranular layers, is not driving but modulatory and may be suppressive (Harris & Mrsic-Flogel, 2013; shown as dashed line in Figure 11a). This connection is not likely to substantially contribute to the present findings.

Visual activity in CDCs reaches the cross-modally reorganized DZ by a corticocortical connection, as indicated by anatomical observations (Barone et al., 2013) and by the latency difference between visual responses in the adjacent visual fields and cross-modal visual responses in DZ (Land et al., 2016). Cross-modal activation recruits a cortical column differently than thalamic input and is rather weak compared to the thalamic auditory drive (Land et al., 2016). It appears probable that this anatomically sparsely distributed weak input might not suffice to activate the cortical column in a coordinated manner and switch infragranular pyramidal neurons into bursting mode (Larkum, Zhu, & Sakmann, 1999), particularly if there was no synchronized input to supragranular and infragranular layers (Larkum, 2013). This may explain why in our study the deep layers show more extensive effects of deafness than the supragranular layers, including areas where a cross-modal function has been previously demonstrated.

5.2.3 | Auditory cortex is active in deafness

In addition to the differences, it is also interesting to consider what deafness does not change: it is surprising how morphologically similar the auditory regions are between deaf and hearing animals, particularly in supragranular layers. To understand this it is important to emphasize that the auditory cortex is not completely silent in congenital deafness: even those neurons that do not become visually taken over show ongoing activity (Land et al., 2016; Tillein, Hubka, & Kral, 2016) that is heavily increased in some sleep stages (Steriade, McCormick, & Sejnowski, 1993). This activity is present even in completely deaf animals (Land and Kral, unpublished). Thus, obviously, complete sensory deprivation does not implicate total silencing of the sensory cortical areas.

Ongoing activity often takes place in the form of cortical propagating waves mediated via local (short-range) connections (Nir et al., 2011; Reimer, Hubka, Engel, & Kral, 2011). Such activity may shape plastic changes (Winnubst, Cheyne, Niculescu, & Lohmann, 2015). Reduced temporal gradients within the auditory cortex together with a more synchronous responsiveness throughout field A1 was observed in CDCs (Kral et al., 2009) that suggest larger divergence and stronger local connectivity in deafness. Developmental studies on the visual system demonstrate that in early development local cortical connectivity is strong and only after onset of experience switches to a patterned long-distance connectivity (Callaway & Katz, 1990; Ko et al., 2013). The present findings are therefore consistent with an immature local pattern of cortical connections that dominate cortical processing in the "deaf" auditory cortex (Figure 11b).

6 | CONCLUSION

The recent findings demonstrate that while general cortical cytoarchitectonic organization is preserved in congenital deafness, anatomical dystrophic effects are observed in deep layers and spread over large cortical regions including the higher-order fields.

ACKNOWLEDGMENTS

The study was supported by Deutsche Forschungsgemeinschaft (Exc 1077).

AUTHOR CONTRIBUTIONS

AK designed the study, DK, VS and AK performed the experiments, DK processed the tissue, CB analyzed the sections and performed statistical comparisons, CB drafted the manuscript, AK finalized the manuscript and the figures, and all authors edited and approved the manuscript.

REFERENCES

Alvarado, J. C., Stanford, T. R., Rowland, B. A., Vaughan, J. W., & Stein, B. E. (2009). Multisensory integration in the superior colliculus requires synergy among corticocollicular inputs. *Journal of Neuroscience*, *29*, 6580–6592.

Bajo, V. M., Nodal, F. R., Moore, D. R., & King, A. J. (2010). The descending corticocollicular pathway mediates learning-induced auditory plasticity. *Nature Neuroscience*, *13*, 253–260.

Barone, P., Lacassagne, L., & Kral, A. (2013). Reorganization of the connectivity of cortical field DZ in congenitally deaf cat. *PLoS One*, *8*, e60093.

Beitel, R. E., Vollmer, M., Raggio, M. W., & Schreiner, C. E. (2011). Behavioral training enhances cortical temporal processing in neonatally deafened juvenile cats. *Journal of Neurophysiology*, *106*, 944–959.

Burkhalter, A., Bernardo, K. L., & Charles, V. (1993). Development of local circuits in human visual cortex. *Journal of Neuroscience*, *13*, 1916–1931.

Butler, B. E., Chabot, N., Kral, A., & Lomber, S. G. (2017). Origins of thalamic and cortical projections to the posterior auditory field in congenitally deaf cats. *Hearing Reseach*, *343*, 118–127.

Butler, B. E., Chabot, N., & Lomber, S. G. (2016). Quantifying and comparing the pattern of thalamic and cortical projections to the posterior auditory field in hearing and deaf cats. *Journal of Comparative Neurology*, *524*, 3042–3063.

Callaway, E. M., & Katz, L. C. (1990). Emergence and refinement of clustered horizontal connections in cat striate cortex. *Journal of Neuroscience*, *10*, 1134–1153.

Campbell, M. J., & Morrison, J. H. (1989). Monoclonal antibody to neurofilament protein (SMI-32) labels a subpopulation of pyramidal neurons in the human and monkey neocortex. *Journal of Comparative Neurology*, *282*, 191–205.

Chabot, N., Mellott, J. G., Hall, A. J., Tichenoff, E. L., & Lomber, S. G. (2013). Cerebral origins of the auditory projection to the superior colliculus of the cat. *Hearing Research*, *300*, 33–45.

Constantinople, C. M., & Bruno, R. M. (2013). Deep cortical layers are activated directly by thalamus. *Science*, *340*, 1591–1594.

Cragg, B. G. (1975a). The development of synapses in kitten visual cortex during visual deprivation. *Experimental Neurology*, *46*, 445–451.

Cragg, B. G. (1975b). The development of synapses in the visual system of the cat. *Journal of Comparative Neurology*, *160*, 147–166.

de la Mothe, L. A., Blumell, S., Kajikawa, Y., & Hackett, T. A. (2006). Cortical connections of the auditory cortex in marmoset monkeys: Core and medial belt regions. *Journal of Comparative Neurology*, *496*, 27–71.

Douglas, R. J., & Martin, K. A. (2004). Neuronal circuits of the neocortex. *Annual Review of Neuroscience*, *27*, 419–451.

Emmorey, K., Allen, J. S., Bruss, J., Schenker, N., & Damasio, H. (2003). A morphometric analysis of auditory brain regions in congenitally deaf adults. *Proceedings of the National Academy of Sciences of the United States of America*, *100*, 10049–10054.

Fallon, J. B., Irvine, D. R., & Shepherd, R. K. (2008). Cochlear implants and brain plasticity. *Hearing Research*, *238*, 110–117.

Fallon, J. B., Irvine, D. R., & Shepherd, R. K. (2009). Cochlear implant use following neonatal deafness influences the cochleotopic organization of the primary auditory cortex in cats. *Journal of Comparative Neurology*, *512*, 101–114.

Fallon, J. B., Shepherd, R. K., Nayagam, D. A., Wise, A. K., Heffer, L. F., Landry, T. G., & Irvine, D. R. (2014). Effects of deafness and cochlear implant use on temporal response characteristics in cat primary auditory cortex. *Hearing Research*, *315*, 1–9.

Finney, E. M., Clementz, B. A., Hickok, G., & Dobkins, K. R. (2003). Visual stimuli activate auditory cortex in deaf subjects: Evidence from MEG. *Neuroreport*, *14*, 1425–1427.

Finney, E. M., Fine, I., & Dobkins, K. R. (2001). Visual stimuli activate auditory cortex in the deaf. *Nature Neuroscience*, *4*, 1171–1173.

Griffiths, T. D., & Warren, J. D. (2004). What is an auditory object? *Nature Reviews Neuroscience*, *5*, 887–892.

Hardie, N. A., Martsi-McClintock, A., Aitkin, L. M., & Shepherd, R. K. (1998). Neonatal sensorineural hearing loss affects synaptic density in the auditory midbrain. *Neuroreport*, *9*, 2019–2022.

Hardie, N. A., & Shepherd, R. K. (1999). Sensorineural hearing loss during development: Morphological and physiological response of the cochlea and auditory brainstem. *Hearing Research*, *128*, 147–165.

Harris, K. D., & Mrsic-Flogel, T. D. (2013). Cortical connectivity and sensory coding. *Nature*, *503*, 51–58.

Hartmann, R., Shepherd, R. K., Heid, S., & Klinke, R. (1997). Response of the primary auditory cortex to electrical stimulation of the auditory nerve in the congenitally deaf white cat. *Hearing Research*, *112*, 115–133.

Heid, S. (1998). Morphologische Befunde am peripheren und zentralen auditorischen System der kongenital gehörlosen weißen Katze. PhD Thesis. Frankfurt am Main. J.W.Goethe University.

Heid, S., Hartmann, R., & Klinke, R. (1998). A model for prelingual deafness, the congenitally deaf white cat–population statistics and degenerative changes. *Hearing Research*, *115*, 101–112.

He, J., & Hashikawa, T. (1998). Connections of the dorsal zone of cat auditory cortex. *Journal of Comparative Neurology*, *400*, 334–348.

Hof, P. R., & Morrison, J. H. (1995). Neurofilament protein defines regional patterns of cortical organization in the macaque monkey visual system: A quantitative immunohistochemical analysis. *Journal of Comparative Neurology*, *352*, 161–186.

Hribar, M., Suput, D., Carvalho, A. A., Battelino, S., & Vovk, A. (2014). Structural alterations of brain grey and white matter in early deaf adults. *Hearing Research*, *318*, 1–10.

Hultcrantz, M., Snyder, R., Rebscher, S., & Leake, P. (1991). Effects of neonatal deafening and chronic intracochlear electrical stimulation on the cochlear nucleus in cats. *Hearing Research*, *54*, 272–280.

Jiang, X., Shen, S., Cadwell, C. R., Berens, P., Sinz, F., Ecker, A. S., ... Tolias, A. S. (2015). Principles of connectivity among morphologically defined cell types in adult neocortex. *Science*, *350*, aac9462.

Kelly, J. P., & Wong, D. (1981). Laminar connections of the cat's auditory cortex. *Brain Research*, *212*, 1–15.

Klinke, R., Kral, A., Heid, S., Tillein, J., & Hartmann, R. (1999). Recruitment of the auditory cortex in congenitally deaf cats by long- term cochlear electrostimulation. *Science*, *285*, 1729–1733.

Ko, H., Cossell, L., Baragli, C., Antolik, J., Clopath, C., Hofer, S. B., & Mrsic-Flogel, T. D. (2013). The emergence of functional microcircuits in visual cortex. *Nature*, *496*, 96–100.

Kok, M. A., Chabot, N., & Lomber, S. G. (2014). Cross-modal reorganization of cortical afferents to dorsal auditory cortex following early- and late-onset deafness. *Journal of Comparative Neurology*, *522*, 654–675.

Kral, A. (2013). Auditory critical periods: A review from system's perspective. *Neuroscience*, *247*, 117–133.

Kral, A., Hartmann, R., Tillein, J., Heid, S., & Klinke, R. (2000). Congenital auditory deprivation reduces synaptic activity within the auditory cortex in a layer-specific manner. *Cerebral Cortex*, *10*, 714–726.

Kral, A., & Lomber, S. G. (2015). Deaf white cats. *Current Biology*, *25*, R351–R353.

Kral, A., Schroder, J. H., Klinke, R., & Engel, A. K. (2003). Absence of cross-modal reorganization in the primary auditory cortex of congenitally deaf cats. *Experimental Brain Research*, *153*, 605–613.

Kral, A., & Sharma, A. (2012). Developmental neuroplasticity after cochlear implantation. *Trends in Neurosciences*, *35*, 111–122.

Kral, A., Tillein, J., Heid, S., Hartmann, R., & Klinke, R. (2005). Postnatal cortical development in congenital auditory deprivation. *Cerebral Cortex*, *15*, 552–562.

Kral, A., Hartmann, R., & Klinke, R. (2006a). Recruitment of the auditory cortex in congenitally deaf cats. In Lomber, S.G., Eggermont, J.J. (Eds.), Reprogramming the cerebral cortex (pp. 191–210). Oxford: Oxford University Press.

Kral, A., Tillein, J., Heid, S., Klinke, R., & Hartmann, R. (2006b). Cochlear implants: Cortical plasticity in congenital deprivation. *Progress in Brain Research*, *157*, 283–313.

Kral, A., Tillein, J., Hubka, P., Schiemann, D., Heid, S., Hartmann, R., & Engel, A. K. (2009). Spatiotemporal patterns of cortical activity with bilateral cochlear implants in congenital deafness. *Journal of Neuroscience*, *29*, 811–827.

Kral, A., Yusuf, P.A., & Land, R. (2017). Higher-order areas in congenital deafness: top-down interactions and corticocortical decoupling. *Hearing Research*, *343*, 50–63.

Land, R., Baumhoff, P., Tillein, J., Lomber, S. G., Hubka, P., Kral, A. (2016). Cross-modal plasticity in higher-order auditory cortex of congenitally deaf cats does not limit auditory responsiveness to cochlear implants. *Journal of Neuroscience*, *36*, 6175–6185.

Larkum, M. (2013). A cellular mechanism for cortical associations: An organizing principle for the cerebral cortex. *Trends in Neurosciences*, *36*, 141–151.

Larkum, M. E., Senn, W., & Lüscher, H. R. (2004). Top-down dendritic input increases the gain of layer 5 pyramidal neurons. *Cerebral Cortex*, *14*, 1059–1070.

Larkum, M. E., Zhu, J. J., & Sakmann, B. (1999). A new cellular mechanism for coupling inputs arriving at different cortical layers. *Nature*, *398*, 338–341.

Leake, P. A., Snyder, R. L., Hradek, G. T., & Rebscher, S. J. (1995). Consequences of chronic extracochlear electrical stimulation in neonatally deafened cats. *Hearing Research*, *82*, 65–80.

Lee, C. C., & Winer, J. A. (2011). Convergence of thalamic and cortical pathways in cat auditory cortex. *Hearing Research*, *274*, 85–94.

Leonard, M. K., Ferjan Ramirez, N., Torres, C., Travis, K. E., Hatrak, M., Mayberry, R. I., & Halgren, E. (2012). Signed words in the congenitally deaf evoke typical late lexicosemantic responses with no early visual responses in left superior temporal cortex. *Journal of Neuroscience*, *32*, 9700–9705.

Li, J., Li, W., Xian, J., Li, Y., Liu, Z., Liu, S., … He, H. (2012). Cortical thickness analysis and optimized voxel-based morphometry in children and adolescents with prelingually profound sensorineural hearing loss. *Brain Research*, *1430*, 35–42.

Lomber, S. G., Meredith, M. A., & Kral, A. (2010). Cross-modal plasticity in specific auditory cortices underlies visual compensations in the deaf. *Nature Neuroscience*, *13*, 1421–1427.

Lustig, L. R., Leake, P. A., Snyder, R. L., & Rebscher, S. J. (1994). Changes in the cat cochlear nucleus following neonatal deafening and chronic intracochlear electrical stimulation. *Hearing Research*, *74*, 29–37.

Markov, N. T., Vezoli, J., Chameau, P., Falchier, A., Quilodran, R., Huissoud, C., … Kennedy, H. (2014). Anatomy of hierarchy: Feedforward and feedback pathways in macaque visual cortex. *Journal of Comparative Neurology*, *522*, 225–259.

McMullen, N. T., & Glaser, E. M. (1988). Auditory cortical responses to neonatal deafening: Pyramidal neuron spine loss without changes in growth or orientation. *Experimental Brain Research*, *72*, 195–200.

McMullen, N. T., Goldberger, B., Suter, C. M., & Glaser, E. M. (1988). Neonatal deafening alters nonpyramidal dendrite orientation in auditory cortex: A computer microscope study in the rabbit. *Journal of Comparative Neurology*, *267*, 92–106.

Mellott, J. G., Bickford, M. E., & Schofield, B. R. (2014). Descending projections from auditory cortex to excitatory and inhibitory cells in the nucleus of the brachium of the inferior colliculus. *Frontiers in Systems Neuroscience*, *8*, 188.

Mellott, J. G., Van der Gucht, E., Lee, C. C., Carrasco, A., Winer, J. A., & Lomber, S. G. (2010). Areas of cat auditory cortex as defined by neurofilament proteins expressing Smi-32. *Hearing Research*, *267*, 119–136.

Meredith, M. A., Clemo, H. R., Corley, S. B., Chabot, N., & Lomber, S. G. (2015). Cortical and thalamic connectivity of the auditory anterior ectosylvian cortex of early-deaf cats: Implications for neural mechanisms of crossmodal plasticity. *Hearing Research*, *333*, 25–36.

Meredith, M. A., & Lomber, S. G. (2011). Somatosensory and visual crossmodal plasticity in the anterior auditory field of early-deaf cats. *Hearing Research*, *280*, 38–47.

Mitani, A., & Shimokouchi, M. (1985). Neuronal connections in the primary auditory cortex: an electrophysiological study in the cat. *Journal of Comparative Neurology*, *235*, 417–429.

Mitani, A., Shimokouchi, M., Itoh, K., Nomura, S., Kudo, M., & Mizuno, N. (1985). Morphology and laminar organization of electrophysiologically identified neurons in the primary auditory cortex in the cat. *Journal of Comparative Neurology*, *235*, 430–447.

Mountcastle, V. B. (1997). The columnar organization of the neocortex. *Brain*, *120*(Pt 4), 701–722.

Mower, G. D., Caplan, C. J., Christen, W. G., & Duffy, F. H. (1985). Dark rearing prolongs physiological but not anatomical plasticity of the cat visual cortex. *Journal of Comparative Neurology*, *235*, 448–466.

Naito, Y., Hirano, S., Fujiki, N., Nishizawa, S., Takahashi, H., Kojima, H., … Honjo, I. (2000). Development and plasticity of the auditory cortex in cochlear implant users: A follow-up study by positron emission tomography. *Advances in Otorhinolaryngology*, *57*, 55–59.

Naito, Y., Hirano, S., Honjo, I., Okazawa, H., Ishizu, K., Takahashi, H., … Konishi, J. (1997). Sound-induced activation of auditory cortices in cochlear implant users with post- and prelingual deafness demonstrated by positron emission tomography. *Advances in Otorhinolaryngology*, *117*, 490–496.

Nir, Y., Staba, R. J., Andrillon, T., Vyazovskiy, V. V., Cirelli, C., Fried, I., & Tononi, G. (2011). Regional slow waves and spindles in human sleep. *Neuron*, *70*, 153–169.

Nishimura, H., Hashikawa, K., Doi, K., Iwaki, T., Watanabe, Y., Kusuoka, H., … Kubo, T. (1999). Sign language 'heard' in the auditory cortex. *Nature*, *397*, 116.

O'Neil, J. N., Limb, C. J., Baker, C. A., & Ryugo, D. K. (2010). Bilateral effects of unilateral cochlear implantation in congenitally deaf cats. *Journal of Comparative Neurology*, *518*, 2382–2404.

Palmer, L. A., Rosenquist, .A C., & Tusa, R. J. (1978). The retinotopic organization of lateral suprasylvian visual areas in the cat. *Journal of Comparative Neurology*, *177*, 237–256.

Petitto, L. A., Zatorre, R. J., Gauna, K., Nikelski, E. J., Dostie, D., & Evans, A. C. (2000). Speech-like cerebral activity in profoundly deaf people processing signed languages: Implications for the neural basis of human language. *Proceedings of the National Academy of Sciences of the United States of America*, *97*, 13961–13966.

Raggio, M. W., & Schreiner, C. E. (1999). Neuronal responses in cat primary auditory cortex to electrical cochlear stimulation. III. Activation patterns in short- and long-term deafness. *Journal of Neurophysiology*, *82*, 3506–3526.

Raizada, R. D., & Grossberg, S. (2003). Towards a theory of the laminar architecture of cerebral cortex: Computational clues from the visual system. *Cerebral Cortex*, *13*, 100–113.

Reale, R. A., & Imig, T. J. (1980). Tonotopic organization in auditory cortex of the cat. *Journal of Comparative Neurology*, *192*, 265–291.

Reale, R. A., Imig, T. J. (1983). Auditory cortical field projections to the basal ganglia of the cat. *Neuroscience*, *8*, 67–86.

Redd, E. E., Cahill, H. B., Pongstaporn, T., & Ryugo, D. K. (2002). The effects of congenital deafness on auditory nerve synapses: Type I and Type II multipolar cells in the anteroventral cochlear nucleus of cats. *Journal of the Association for Research in Otolaryngology*, *3*, 403–417.

Reimer, A., Hubka, P., Engel, A. K., & Kral, A. (2011). Fast propagating waves within the rodent auditory cortex. *Cerebral Cortex*, *21*, 166–177.

Rose, J. E. (1949). The cellular structure of the auditory region of the cat. *Journal of Comparative Neurology*, *91*, 409–439.

Rubin, J., Ulanovsky, N., Nelken, I., & Tishby, N. (2016). The representation of prediction error in auditory cortex. *PLoS Computational Biology*, *12*, e1005058.

Ryugo, D. K., Rosenbaum, B. T., Kim, P. J., Niparko, J. K., & Saada, A. A. (1998). Single unit recordings in the auditory nerve of congenitally deaf white cats: Morphological correlates in the cochlea and cochlear nucleus. *Journal of Comparative Neurology*, *397*, 532–548.

Saada, A. A., Niparko, J. K., & Ryugo, D. K. (1996). Morphological changes in the cochlear nucleus of congenitally deaf white cats. *Brain Research*, *736*, 315–328.

Schofield, B. R. (2009). Projections to the inferior colliculus from layer VI cells of auditory cortex. *Neuroscience*, *159*, 246–258.

Sento, S., & Ryugo, D. K. (1989). Endbulbs of held and spherical bushy cells in cats: Morphological correlates with physiological properties. *Journal of Comparative Neurology*, *280*, 553–562.

Stakhovskaya, O., Hradek, G. T., Snyder, R. L., & Leake, P. A. (2008). Effects of age at onset of deafness and electrical stimulation on the developing cochlear nucleus in cats. *Hearing Research*, *243*, 69–77.

Steriade, M., McCormick, D. A., & Sejnowski, T. J. (1993). Thalamocortical oscillations in the sleeping and aroused brain. *Science*, *262*, 679–685.

Sternberger, L. A., & Sternberger, N. H. (1983). Monoclonal antibodies distinguish phosphorylated and nonphosphorylated forms of neurofilaments in situ. *Proceedings of the National Academy of Sciences of the United States of America*, *80*, 6126–6130.

Suga, N., & Ma, X. (2003). Multiparametric corticofugal modulation and plasticity in the auditory system. *Nature Reviews Neuroscience*, *4*, 783–794.

Symonds, L. L., & Rosenquist, A. C. (1984). Corticocortical connections among visual areas in the cat. *Journal of Comparative Neurology*, *229*, 1–38.

Tillein, J., Hubka, P., & Kral, A. (2016). Monaural congenital deafness affects aural dominance and degrades binaural processing. *Cerebral Cortex*, *26*, 1762–1777.

Tillein, J., Hubka, P., Syed, E., Hartmann, R., Engel, A. K., & Kral, A. (2010). Cortical representation of interaural time difference in congenital deafness. *Cerebral Cortex*, *20*, 492–506.

van der Gucht, E., Vandesande, F., & Arckens, L. (2001). Neurofilament protein: A selective marker for the architectonic parcellation of the visual cortex in adult cat brain. *Journal of Comparative Neurology*, *441*, 345–368.

Voigt MB, Hubka P, Kral A. 2017. Intracortical microstimulation differentially activates cortical layers based on stimulation depth. *Brain Stimulation*, *10*, 684–694.

Winer, J. A. (1984a). The non-pyramidal cells in layer III of cat primary auditory cortex (AI). *Journal of Comparative Neurology*, *229*, 512–530.

Winer, J. A. (1984b). The pyramidal neurons in layer III of cat primary auditory cortex (AI). *Journal of Comparative Neurology*, *229*, 476–496.

Winer, J. A. (1992). The functional architecture of the medial geniculate body and the primary auditory cortex. In Webster, D. B., Popper, A. N., & Fay, R. R. (Eds.), The mammalian auditory pathway: Neuroanatomy (pp. 222–409). New York: Springer.

Winer, J. A., & Lee, C. C. (2007). The distributed auditory cortex. *Hearing Research*, *229*, 3–13.

Winer, J. A., & Prieto, J. J. (2001). Layer V in cat primary auditory cortex (AI): Cellular architecture and identification of projection neurons. *Journal of Comparative Neurology*, *434*, 379–412.

Winfield, D. A. (1981). The postnatal development of synapses in the visual cortex of the cat and the effects of eyelid closure. *Brain Research*, *206*, 166–171.

Winfield, D. A. (1983). The postnatal development of synapses in the different laminae of the visual cortex in the normal kitten and in kittens with eyelid suture. *Brain Research*, *285*, 155–169.

Winnubst, J., Cheyne, J. E., Niculescu, D., & Lohmann, C. (2015). Spontaneous activity drives local synaptic plasticity in vivo. *Neuron*, *87*, 399–410.

Wong, C., Chabot, N., Kok, M. A., & Lomber, S. G. (2013). Modified areal cartography in auditory cortex following early- and late-onset deafness. *Cerebral Cortex*, *24*, 1778–1792.

Xiong, X. R., Liang, F., Zingg, B., Ji, X. Y., Ibrahim, L. A., Tao, H. W., & Zhang, L. I. (2015). Auditory cortex controls sound-driven innate defense behaviour through corticofugal projections to inferior colliculus. *Nature Communications*, *6*, 7224.

Znamenskiy, P., & Zador, A. M. (2013). Corticostriatal neurons in auditory cortex drive decisions during auditory discrimination. *Nature*, *497*, 482–485.

How to cite this article: Berger C, Kühne D, Scheper V, Kral A. Congenital deafness affects deep layers in primary and secondary auditory cortex. *J Comp Neurol*. 2017;525:3110–3125. https://doi.org/10.1002/cne.24267